Coexisting Phenomena of Surge and Rotating Stall in an Axial Flow Compressor

Takuya ABE[1], Hiroaki MITSUI[1] and Yutaka OHTA[2]

1. Graduate Student, Graduate School of Science and Engineering, Waseda University, 3-4-1 Okubo, Shinjuku, Tokyo 169-8555, Japan
2. Department of Applied Mechanics and Aerospace Engineering, Waseda University, 3-4-1 Okubo, Shinjuku, Tokyo 169-8555, Japan

The unsteady inner flow structure of a single-stage axial flow compressor under the coexisting conditions of surge and rotating stall was experimentally investigated via detailed measurements of the unsteady characteristics and the internal flow velocity fluctuations. The main relevant feature of the tested compressor is a shock tube with a capacity tank connected in series to the compressor outlet through slits and a concentric duplex pipe: surge and rotating stall can both be generated by connecting the shock tube. Research attention is focused on the unsteady behavior of a rotating stall during the surge cycle. The size of the rotating stall cell during the recovery process of an irregular surge cycle was experimentally determined by the circumferential flow velocity fluctuations ahead of the rotor blade. The results suggested that the size of the rotating stall cell at the switching point of the performance curve between large and small cycles is considered to be the key parameter in determining the following surge cycle. In addition, the surge cycle is largely influenced by the unsteady behavior of the rotating stall cell.

Keywords: Axial flow compressor, Surge, Rotating stall, Coexisting state of surge and rotating stall

Introduction

The internal flow of turbomachinery, including axial flow compressors, is inherently unsteady. The causative fluctuation concerns a number of complicated processes, such as the interference by a strut or cascade wake flow with downstream cascades, potential interference between cascades, self-induced oscillation of a cascade flutter, flow separation on the blade surface and the flow passage wall, interference by a non-uniform flow within the cascade, the rotating stall within the cascade, and the surge in addition to the turbulence of the flow itself. In particular, the surge and the rotating stall are well known as distinct phenomena generated in axial flow compres-sor systems and many reports on them have been pub-lished [1].

Surge is an axial-direction instability generated by self-induced oscillations, which is caused by the negative resistance of the compressor system. Surge interferes with the transient characteristics of the fluid in the duct, and violently fluctuates with respect to pressure and mass flow with a low eigenfrequency. Therefore, surge is often called a "global instability" [2, 3]. The rotating stall is a circumferential-direction instability. The low energy re-gion, i.e., the stall cell, originates in a local flow separa-tion on the blade surface at low flow rates and rotates in a circumferential direction at approximately half of the rotor speed. Because of these characteristics, the rotating

stall is often called a "local instability" [4,5]. The surge and the rotating stall, which have different characteristics and occurrence factors, are considered to be independent oscillating phenomena. A compressor reaches instability through different processes depending on the mechanical characteristics of the conduit system. The oscillating phenomena depend on the ratio of the Helmholtz resonator frequency to the frequency of the rotating stall. This ratio is called Greitzer's B parameter, and the experimental results indicate that the critical value of the B parameter, which classifies the surge and the rotating stall, is approximately 0.8 for an axial flow compressor [6].

However, Tryfonidis et al. [7] and Garnier et al. [8] indicated by detailed experiments and numerical simulations that the "local instability" is generated prior to the "global instability"; in fact, it plays an important role as a precursory phenomenon to the surge. Meanwhile, McCaughan et al. [9] examined the bifurcation phenomena of the surge and the rotating stall, and determined that the boundary is not only affected by the B parameter, but also altered depending on the compressor characteristics and the variations of the operating point. The study on the interactions between the surge and the rotating stall with the coexisting system next progressed to the following studies: a Greitzer-Moore model analysis [11, 12]; the correlation between the compressor total-to-static pressure-rise characteristics; and the analytical approach of the estimate of these two phenomena [13].

However, the mutual relations among the coexisting conditions, surge, and rotating stall from the view-point of inner flow structure and behavior have not yet been investigated in detail.

Therefore, an expandable-stage axial-flow compressor, which has a shock tube that includes a capacity tank connected in series to a compressor outlet, was used in order to investigate the various types of coexisting phenomena due to surge and rotating stall by measuring the unsteady characteristics and the internal flow velocity. In the experiments, the size of the rotating stall cell was investigated by using the circumferential flow velocity ahead of the rotor blade during the surge cycle for the case of the "irregular cycle," and the determining factor of the surge cycle was experimentally detected.
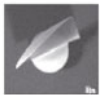
Experimental Procedure

Experimental apparatus

The transient phenomena were investigated using the testing compressor, which connects downstream to a shock tube equipped with a capacity tank. The outlines of the experimental apparatus and measurement system are shown in Fig.1, and the design features of the rotor blades and the stator vanes are listed in Table 1.
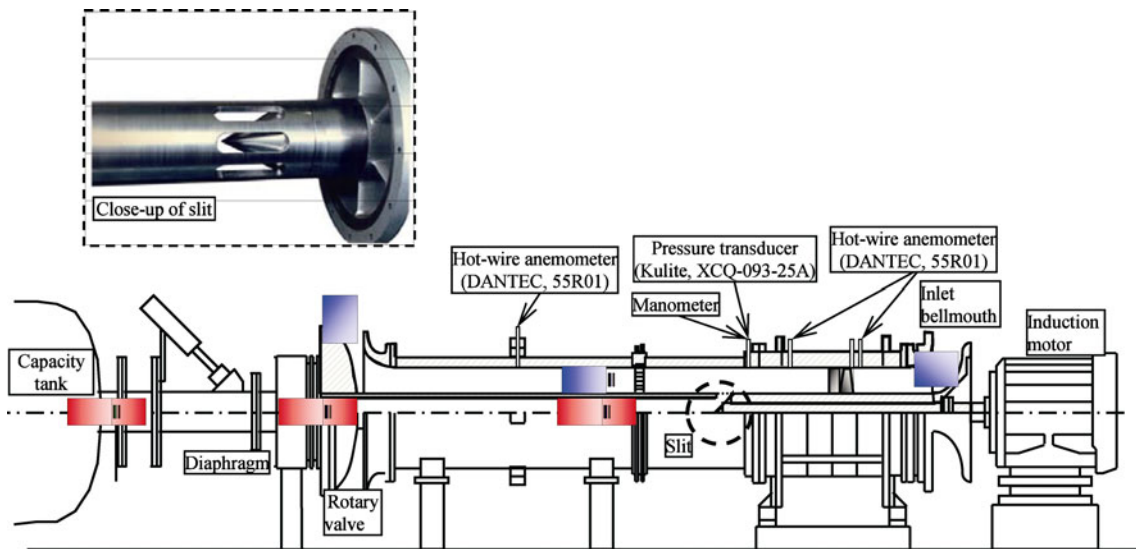
Fig.1 Experimental apparatus and measuring system.

Table.1 Design features of rotor and stator.

Blade	Stagger angle (at hub)	Stagger angle (at tip)	Rn	Sn
Rn	30.798 deg	64.061 deg		
Sn	16.844 deg	9.9992 deg		

The compressor is an axial-flow compressor that can expand from one to three stages, and the number of rotor blades and stator vanes is 12 and 15, respectively. The rotor setting angle can vary from −25° to 25° in increments of 5°, and the stator stagger angle can also be set independently from 30° to −30° according to design

specifications. The tested rotational speed is 12000 min^{-1}, and the operating point is adjusted by the rotary valve set on the exit duct. The main feature of the compressor is a shock tube with a capacity tank of 0.262 m^3 that is connected in series to the compressor outlet through eight slits and a concentric duplex pipe, depicted in Fig.1. The compressor can be connected to a shock tube by removing the diaphragm, thereby generating the coexisting states of surge and rotating stall.

Measurement methods

The compressor performance was obtained using the data for the pressure-rise characteristics and the axial velocities. As indicated in Fig.1, the steady-state pressure-rise characteristics of the compressor were measured using a static manometer and a one-dimensional single hot-wire anemometer (DANTEC, 55R01), both installed in the exit duct. The unsteady pressure fluctuations were measured using a precision pressure transducer (Kulite, XCQ-093-25A) installed at the same point as the manometer, whereas the velocity was measured using the one-dimensional hot-wire anemometer placed behind the stator vane. The inner flow structure of the compressor was investigated via the internal flow velocity fluctuation data obtained by the one-dimensional hot-wire anemometer set 5 mm ahead of the rotor blade's leading edge.

For more information about the testing compressor system and experimental methods, please refer to a related paper [14].

Basic Characteristics of Compressor and Coexisting States of Surge and Rotating Stall

Compressor stall characteristics

The steady-state performance curves, measured when the diaphragm installed in the outlet duct and the testing compressor was disconnected from the shock tube, are shown in Fig.2 by black circles. The flow coefficient ϕ and the total pressure-rise coefficient ψ in the figure are defined as follows:

$$\varphi = C_x / U \quad , \quad \psi_{total} = 2p_t / (\rho U^2) \qquad (1)$$

where C_x is the time-averaged axial velocity, U is the rotor tip speed (81.68 m/s), p_t is the total pressure rise, and ρ is the air density.

The design operating point of the compressor is at $\phi = 0.360$, which is shown by blue circles in the figure. The testing compressor typically stalled in two steps, as shown in Fig.2(d). The first step is considered "mild stall," in which only one stall cell generated near the rotor tip region rotates at approximately 65% of the rotor tip velocity. Further throttling the mass flow rate induced the second stall step, called "deep stall," where the stall

cells expand toward the rotor hub region and generate a full-span stall.
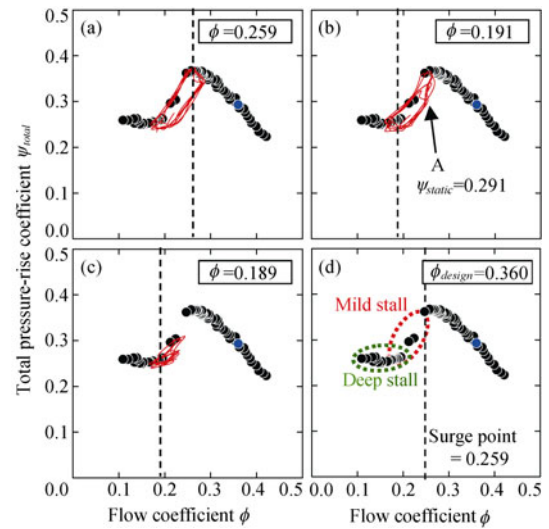
Fig.2 Unsteady behavior of tested compressor under coexistence state of surge and rotating stall.

Unsteady behavior of surge

When the compressor was connected to the capacity tank, the coexisting phenomena of surge and rotating stall were generated. Fig.2(a) to (c) shows the different types of surge cycles achieved by throttling the mass flow rate gradually when opening the diaphragm

Unstable phenomena were not observed until $\phi = 0.259$, when the compressor began operating on the negative slope region of the performance curve. The compressor then abruptly rushed into a deep surge, accompanied by large pressure and mass flow fluctuations when the flow coefficient reaches $\phi = 0.259$. Then, the surge behavior began changing irregularly; three types of surge cycles are typically observed, as indicated in Fig.2(a) to (c). When the flow coefficient was set to $\phi = 0.259$, as shown in Fig.2(a), a "large cycle" occurred and unsteady operating points oscillated back and forth between stable operation and deep stall regions. When the flow coefficient was set to $\phi = 0.189$, as shown in Fig.2(c), a "small cycle" occurred and unsteady operating points oscillated back and forth between the mild stall and the deep stall regions. Two types of surge cycles are selected irregularly ("irregular cycle") when the mass flow rate is set between these two flow rates and $\phi = 0.191$. In the irregular cycle, the operating point $\psi_{static} = 0.291$, shown by A in Fig.2(b), was defined as the switching point between "large" and "small" cycles.

Interactions between Surge and Rotating Stall

Size of stall cell for mild stall condition

The size of the rotating stall cell was investigated ex-

perimentally in order to detect the determining factor of the surge cycle for the "irregular cycle" shown in Fig.2(b). First, the size of the stall cell in the mild stall region was investigated when the compressor was disconnected from the capacity tank.

Fig.3 shows the span-wise distribution of the time histories of circumferential flow velocities ahead of the rotor blade (hereafter abbreviated as ARB) for the mild stall condition, $\phi = 0.248$. The passage of the stall cell can be easily detected by the circumferential flow velocity fluctuations because the swirling flow emerges in order to avoid the stall cell. The fluctuations were more notably captured in the tip region than in the hub region. Frequency analyses of the velocity fluctuations show there is a discrete peak component at 106.9 Hz, which is considered the rotational period of the stall cell, as shown in Fig.3.
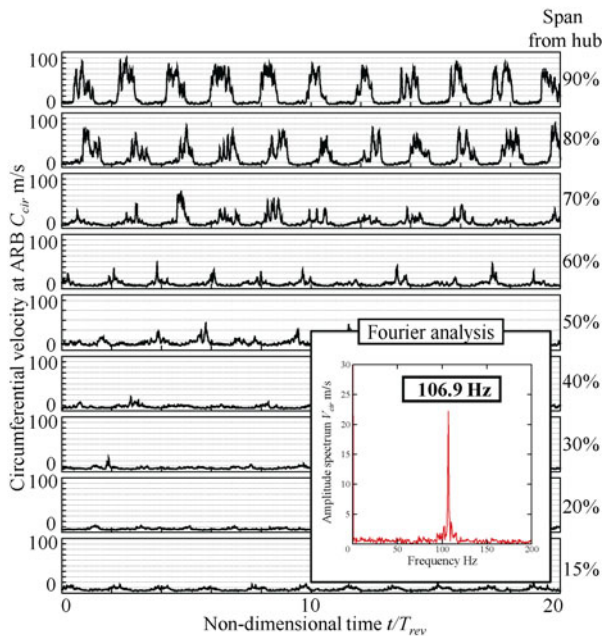

Fig.3 Spanwise Distribution of circumferential flow velocity.

In order to investigate the size of the stall cells, two assumptions about the stall cell were made. First, the stall cell does not generate, disappear, merge, or separate abruptly. Second, the rotational speed of the stall cell remains constant.

Fig.4 shows a typical example of an investigation of the stall cell size at 90% span from the hub. The left figures are cross-sectional views at ARB and the red regions represent the assumed stall cells. The right figures are the time histories of the circumferential flow velocity at ARB. The circumferential velocity increased when the stall cell reached the measuring point defined at time $t = t_0$. Then, the velocity recovered to the original state when the stall cell passed through the measuring point completely at $t = t_1$. After that, the stall cell circled back to the measuring

point again at $t = t_2$. By using these time values, the circumferential extend of the stall cell (abbreviated as EC) at a 90% span from the hub was calculated as follows:

$$EC = \frac{t_1 - t_0}{t_2 - t_0}\% \qquad (2)$$

where $t_1 - t_0$ is the time interval of the stall cell passing through the measuring point and, $t_2 - t_0$ is the rotational period of the stall cell (1/106.9 s).
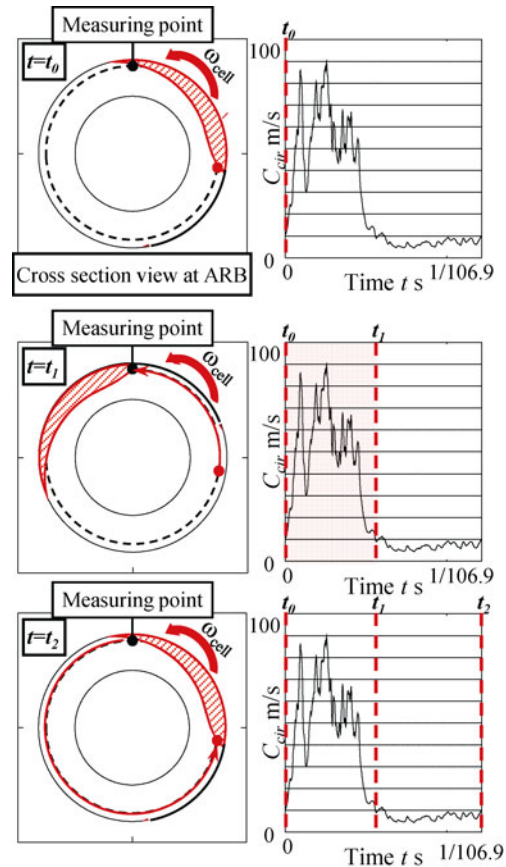

Fig.4 Investigation of the extent of stall cell

By calculating the EC value at 9 points in the span-wise direction, the extent of the stall cell can be estimated, as shown in Fig.5. The experimental results are the average of 100 stall cell measurements. This result indicates that the extent of stall cell is the largest in the tip region and diminishes gradually in the span-wise direction toward the hub, as previously pointed out [15]. By considering both this result and the previous reports on the stall cell shape by Das et al. [16] and Poensgen et al .[17], the extent of the stall cell at each span was determined and is represented as the red strip shape shown in Fig.6. Furthermore, in order to evaluate the influence of the flow blockage on the rotor cascade, the blockage ratio (abbreviated as BR) was defined as follows:
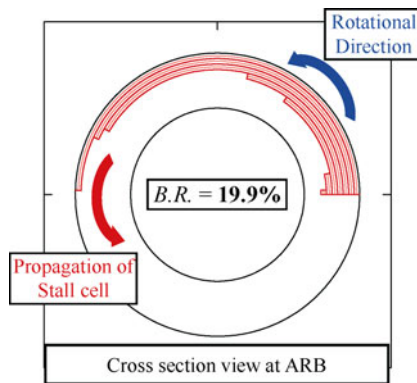
$$BR = \frac{A_{Blockage}}{A_c} \times 100\% \qquad (3)$$

where $A_{Blockage}$ is the summation of the red strip area at each span and A_c is the flow passage area at ARB (8.45 × 10^{-3} m^2).

For a mild stall condition, the calculated BR was 19.9%, as shown in Fig.6.
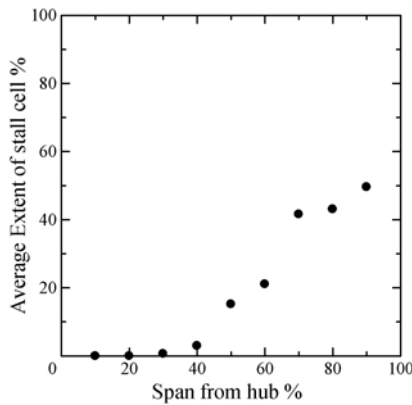
Fig.5 Spanwise distribution of circumferential extend of stall cell.


**Fig.6** Cross section view of stall cell in mildstall regions.

Size of stall cell during the surge cycle

The size of the rotating stall cell during the "irregular cycle" was investigated using the same method as mentioned above. The red traces in Fig.7 show an irregular surge cycle when the compressor is connected to the capacity tank. The unsteady operating point during the recovery process of large and small cycles shows the same trace just before the switching point A shown in the figure. Therefore, in order to investigate the determining factor of the surge cycle, which is assumed to exist during the recovery process, the size of the rotating stall cell was investigated. The blue circle plots in Fig.7 indicate the operating points recovering from a deep stall to a stable operation region, when the compressor was disconnected from the capacity tank. The frequency analyses of the circumferential velocities at ARB of each of

the operating points show a discrete peak component of 106.5 Hz in Fig.8, and therefore, the rotational frequency of the rotating stall cell during the surge cycle was determined to be 106.5 Hz.
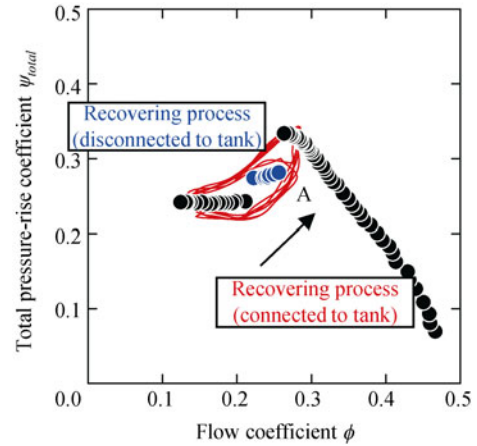

Fig.7 Irregular surge cycle and unsteady operating points in the recovering process.
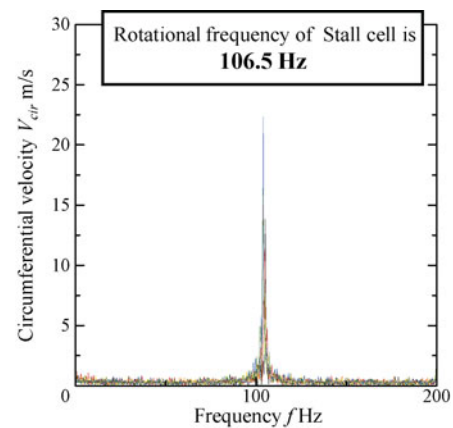
Fig.8 Fourier Analysis of the circumferential velocity measured at ARB during the surge recovering process.

The size of the rotating stall cell during an irregular surge cycle was investigated for four cases of cycles changing: large cycle to large cycle (L-L cycle); large cycle to small cycle (L-S cycle); small cycle to large cycle (S-L cycle); and small cycle to small cycle (S-S cycle). Fig.9 presents a typical example of the investigation of the stall cell size during an L-L cycle. The time histories of the static pressure-rise coefficient ψ_{static} and the circumferential flow velocity C_{cir} measured at 90% span from the hub are shown in Fig.9(a), and the corresponding surge behavior is shown in Fig.9(b) by a thick red trace. The passage of the rotating stall cell can be easily detected by the fluctuation of the circumferential flow velocity, as shown in Fig.9. The EC value of the rotating stall cell was calculated using Eq. (2) in which $t_2 - t_0$ is set to 1/106.5 s. The corresponding unsteady operating
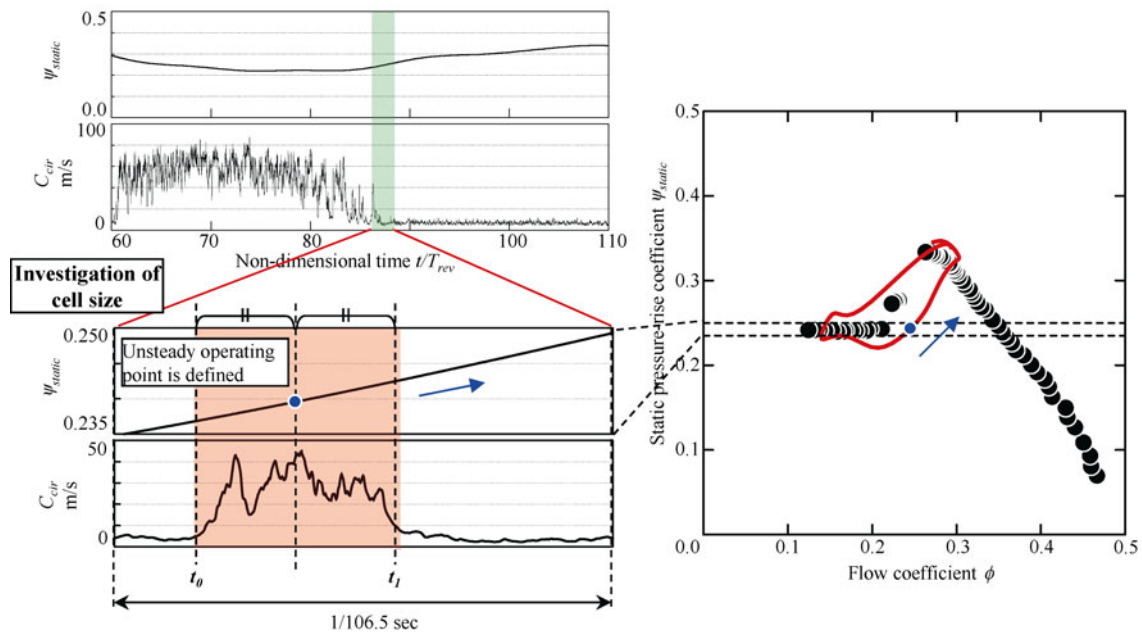
(a) Time histories of static pressure and circumferential velocity.   (b) Definition of unsteady operating point during surge cycle.

Fig.9   Investigation of the size of rotating stall cell in L-L surge cycle.

point was defined as the ψ_{static} value at the midpoint of the time interval of the rotating stall cell and is indicated by the blue circles in the figure.

By calculating the *EC* values during the recovery processes of 10 surge cycles and at 9 points in the span-wise direction, the extent of the rotating stall cell at each span during the surge recovery process was estimated, as shown in Fig.10. Each approximate curve of an *EC* value was drawn with the least squares method from the experimental results. The investigation of the size of the rotating stall cell was omitted at the locations less than 50% span from the hub, because the passage of the rotating stall cell cannot be detected from the velocity fluctuation data for these cases. This result indicates that
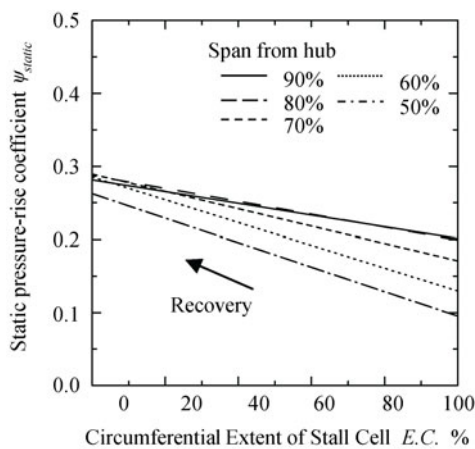
Fig.10   Spanwise variation of expansion ratio of rotating stall cell (L-L cycle).

the extent of the stall cell is larger and the speed of stall cell shrinkage is slower for the tip region than for the hub region, as expected.

Through interpretation of these results, the extent of the rotating stall cell at each span during the recovery processes for the four cases was determined and is represented by the red strip shape shown in Fig.11. Furthermore, by using Eq. (3), the flow blockage ratio within the rotor cascade during the recovery process can be calculated, as shown in Fig.12. The size of the rotating stall cell was investigated at three operating points from A to C shown in Fig.12. The static pressure-rise coefficient of each operating points are ψ_{static} = 0.291 (switching point), 0.251, and 0.219. The size of the rotating stall cell was reduced while recovering the static pressure. As shown by A_1 and A_2 in the figure, the rotating stall cell was eliminated when the following surge cycle was large (i.e., L-L and S-L cycles) at the moment the compressor operating point passed the switching point A. Conversely, the rotating stall cell still remained when the following surge cycle was small (i.e., L-S and S-S cycles) as shown by A_3 and A_4. This result suggests that the size of the rotating stall cell at the switching point A is considered to be the key parameter in determining the following surge cycle. The surge behavior moves to the mild stall region without returning to the stable operation region because the flow blockage is generated by the remaining stall cell.

Conclusions

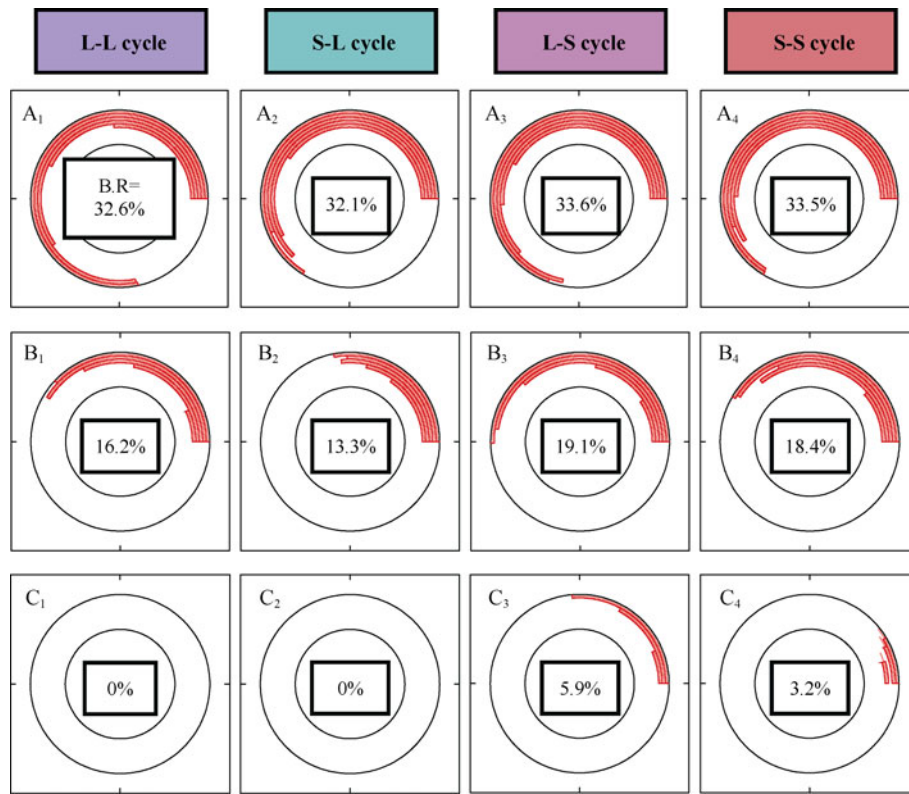The unsteady behavior of a rotating stall cell during a surge cycle in a single-stage axial flow compressor was

Fig. 11   Size of rotating stall cell and flow blockages in various surge cycles.
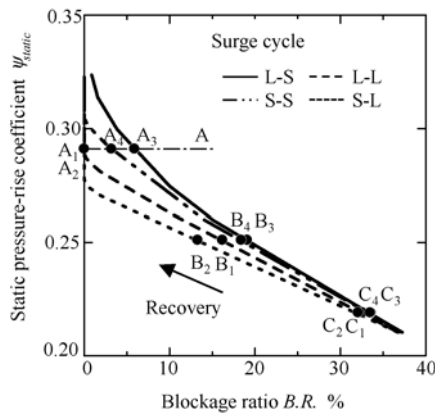

Fig. 12   Comparison of rotor blockage ratio by four surge cycles.

investigated by detailed measurements of the unsteady performance curve and circumferential flow velocity fluctuations at ahead of the rotor blade. The extent of the stall cell, which was experimentally determined by precise measurements of unsteady velocity fluctuations, was the largest in the tip region and diminished gradually in the span-wise direction for the hub when the tested compressor was disconnected from the capacity tank. The extent of the stall cell was larger and the speed of stall cell shrinkage was slower in the tip region than in the hub region during the surge recovery process. The flow

blockage ratio within the rotor cascade during the surge recovery process indicates that the size of the rotating stall cell at the switching point between "large" and "small" cycles is the key parameter in determining the following surge cycle. As a result, the unsteady behavior of the rotating stall cell and corresponding flow blockage within the rotor cascade had profound influence on the unsteady behavior of the irregular surge cycle.

References

[1]   Emmons, H. W., Pearson, C. E., and Grant, H. P.: Compressor Surge and Stall Propagation, Trans. ASME, 77, p.455 (1955).

[2]   Cumpsty, N. A. and Greitzer, E. M.: A Simple Model for Compressor Stall Cell Propagation, Trans. ASME, J. of Eng. For Power, 104, p.170 (1982).

[3]   Day, I. J and Cumpsty, N. A.: The Measurement and Interpretation of Flow within Rotating Stall Cells in Axial Compressors", J.Mech.Engeneering, Sci. IMechE 20-2, p.101 (1978).

[4]   Greitzer, E. M.: Surge and Rotating Stall in Axial Flow Compressors, Part I: Theoretical Compression System Model, Trans. ASME, J. of Eng. For Power, vol.98, No.2, p.190 (1976).

[5]   Greitzer, E. M.: Surge and Rotating Stall in Axial Flow

Compressors, Part II: Experimental Results and Comparison with Theory, Trans. ASME, J. of Eng. For Power,

[6]　Greitzer, E. M.: The Stability of Pumping Systems-1980 Freeman Scholar Lectures, Trans. ASME, J. of Fluids Eng., vol.103, No.2, p.193 (1981).

[7]　Tryfonidis, M., Etchever, O., Paduano, J.D. Epstein, A.H. and Hendrics, G. J.: Prestall Behavior of Several High Speed Compressors, Trans. ASME, J. Turbomachinery, 117, p.62 (1995).

[8]　Garnier, V. H., Epstein, A. H., and Greitzer, E. M.: Rotating Waves as a Stall Inception Indication in Axial Compressors, Trans. ASME, J. of Turbomachinery, vol.113, p.290 (1991).

[9]　McCaughan, F. E.: Application of Bifurcation Theory to Axial Flow Compressor Instability, Trans. ASME, J. Turbomachinery, vol.111, p.426 (1989).

[10]　McCaughan, F. E.: Numerical Results for Axial Flow Compressor Instability, Trans. ASME, J. Turbomachinery, vol.111, p.434 (1989).

[11]　Moore, F. K. and Greitzer, E. M.: A Theory of Post- Stall Transients in Axial Compression Systems: Part I-Development of Equations, Trans. ASME, J. of Eng., For Gas

Turbines and Power, vol.108, p.68 (1986).

[12]　Moore, F. K. and Greitzer, E. M.: A Theory of Post- Stall Transients in Axial Compression Systems: Part II-Application, Trans. ASME, J. of Eng., For Gas Turbines and Power, vol.108, p.231 (1986).

[13]　Ishii, H., Kashiwabara, Y.: Study on Surge and Rotating Stall in Axial Compressors, 1st Report, A Summary of the Measurement and Fundamental Analysis Method, Trans. JSME(B), 54−503, p.1669 (1989).

[14]　Y. Fujita, T. Abe, K. Miyagawa, Y. Ohta.: Stability Enhancement of Axial-Flow Compressor by Jet Injection, ISFMFE2012, Jeju Island, Korea, (2012).

[15]　E. Outa, Y. Outa, D. Kato and K. Chiba: Two-dimensional Study on Evolution of Deep Rotating Stall under Uniform and Stationary Distorted Inlet Flow Conditions, Proc, 14th ISABE, Florence, Italy, p.1 (1999).

[16]　Das, D.K., Jiang, H.K.: An Experimental Study of Rotating Stall in a Multistage Axial-Flow Compressor, ASME, J. of Eng., For Gas Turbines Power, vol.106, p.542 (1984).

[17]　Poensgen, C.A., Gallus, H.E.: Rotating Stall in a Single-Stage Axial Flow Compressor, ASME, J of Turbomachinery, vol.118, p.189 (1996).